

Superconductivity in the Two-Orbital Hubbard Model of Infinite-Layer Nickelates

Zhihui Luo, Dao-Xin Yao,* and Wéi Wú†

Center for Neutron Science and Technology, Guangdong Provincial Key Laboratory of Magnetoelectric Physics and Devices, School of Physics, Sun Yat-sen University, Guangzhou, Guangdong Province 510275, China

(Dated: October 20, 2023)

The pairing symmetry in infinite-layer nickelate superconductors has been an intriguing problem under heated debates. In this work, we study a two-orbital Hubbard model with one strongly correlated $3d$ orbital and one more itinerant $5d$ orbital, by using an eight-site cellular dynamic mean field theory study. We establish a superconducting phase diagram with $d_{x^2-y^2}$, s_{\pm} and $d+is$ wave pairing symmetries, based on which we clarify the roles of various relevant parameters including hybridization V , itinerant carrier density $\langle n_c \rangle$ and interaction U_c . We show that the inclusion of a less correlated $5d$ band in general suppresses the $d_{x^2-y^2}$ wave pairing. We demonstrate that the $d+is$ wave is maximized when the $5d$ orbital has a large Coulomb repulsion with intermediate hybridization parameter. We perform fluctuation diagnostics to show that the driving force behind the $d_{x^2-y^2}$ wave is the intraband antiferromagnetic fluctuations in the $3d$ orbital, while for the s_{\pm} wave, the pairing is mainly from the antiferromagnetic correlations residing on the local $3d$ - $5d$ bond in real space.

I. INTRODUCTION

Identifying the predominant pairing symmetry is a fundamental problem in the study of unconventional superconductors which is usually rooted in comprehending the intricate underlying mechanism of electron pairings. In the case of cuprate superconductors, the spin-singlet pairing with $d_{x^2-y^2}$ wave symmetry dominates the superconducting (SC) phase diagram, which is linked to doping a Mott insulator on an effective single band two-dimensional square lattice [1]. In iron-based superconductors (FeSC), s_{\pm} wave pairing is ubiquitous in various compounds, due to the multi-orbital physics of the intricate Fe- $3d$ orbitals at the Fermi energy (E_F) that favours the inter-band s_{\pm} wave pairing. It is notable that in some pnictides or chalcogenides, a proximate $d_{x^2-y^2}$ wave pairing may also be possible [2, 3] when adjusting the pnictogen height [4] or doping [5].

Experimentlists recently discovered a new class of nickelate-based superconductors $\mathcal{R}\text{NiO}_2$ (\mathcal{R} represents rare-earth element La, Pr or Nd) [6–16]. Despite hosting a relative low SC transition temperature (T_c) (~ 10 K), the nickelate-based superconductors are widely believed to have profound theoretical implications for the field of unconventional superconductivity, given its analog to cuprate superconductors and its strong-coupling nature. Concerning the pairing symmetry, both nodal and nodeless, or even nodal+nodeless gaps [9, 17, 18] have been reported in tunneling or London penetration measurements, implying a possible coexistence of $d_{x^2-y^2}$ and s_{\pm} wave pairings. Subsequently, a theoretical conjecture was proposed [19] which suggests the existence of a crucial Kondo exchange in nickelates that drives the pairing symmetry towards the nodeless s_{\pm} wave. This proposal points to a multi-orbitals nature of the low-energy

physics of nickelates. Meanwhile, there is also evidence indicating that nickelates have a rather large charge-transfer energy within the Zaanen-Sawatzky-Allen (ZSA) scheme [20–24], which means that, to some extent, nickelates may behave as a single-band doped Mott insulator, much like the cuprates. Nevertheless, the undoped nickelates in fact exhibit weak insulating characteristics [7, 8, 10, 14] which may be explained as the self-doping effect via the Kondo couplings [25] between the \mathcal{R} - $5d$ states and the 2D hole band of Ni- $3d_{x^2-y^2}$ orbital [23, 26]. On the other hand, density functional theory plus dynamical mean-field theory (DFT+DMFT) calculations also emphasize a crucial multi-orbital description of the nickelates [27–32].

The intriguing phenomena of nickelates have attracted much attention to a very basic question: how the pairing symmetry is determined in a two-dimensional interacting electron system that has both strongly and less correlated bands (such as the Ni- $3d_{x^2-y^2}$ and \mathcal{R} - $5d$ orbitals in nickelates respectively)? Specifically, as the hybridization strength V between the two bands changes, the geometry of Fermi surface (FS) would change accordingly, leading to the immediate alteration of the free energy of the pairing state with certain symmetry. A subsequent question then prompts that whether the geometry of FS is the only important factor in determining the symmetry of pairing [33]? To address these questions, we study a doped two-band Hubbard model to establish a phase diagram describing the evolution trajectory of the pairing symmetries. We also explore the dependence of the superconducting T_c of $d_{x^2-y^2}$ and s_{\pm} wave pairing on various parameters, such as the strength of the Hubbard U at both bands, the filling factor (n), etc. Moreover, we search in the parameter space for the possible coexistence of the $d_{x^2-y^2}$ and s_{\pm} wave instability, namely, the $d+is$ wave. We find that it only exists when the two correlated bands both have a relatively large U and in the intermediate V regime. Finally, we perform fluctuation diagnostics analysis in the superconducting phases,

* Corresponding author: yaodaox@mail.sysu.edu.cn

† Corresponding author: wuwei69@mail.sysu.edu.cn

which reveals that the $d_{x^2-y^2}$ and s_{\pm} wave pairing symmetries have different origin of pairing: the $d_{x^2-y^2}$ wave is largely driven by the (π, π) antiferromagnetic fluctuations whereas for s_{\pm} pairing, is more from local in real-space inter-band antiferromagnetic fluctuations.

II. MODEL AND METHODS

We consider the two-orbital Hubbard model that reads [34–45]

$$\begin{aligned} \mathcal{H} = & \sum_{\mathbf{k}\sigma} (t_{\mathbf{k}}^d - \mu^d) d_{\mathbf{k}\sigma}^{\dagger} d_{\mathbf{k}\sigma} + \sum_{\mathbf{k}\sigma} (t_{\mathbf{k}}^c - \mu^c) c_{\mathbf{k}\sigma}^{\dagger} c_{\mathbf{k}\sigma} \\ & + V \sum_{\mathbf{k}\sigma} \left(d_{\mathbf{k}\sigma}^{\dagger} c_{\mathbf{k}\sigma} + h.c. \right) \\ & + U_d \sum_i n_{i\uparrow}^d n_{i\downarrow}^d + U_c \sum_i n_{i\uparrow}^c n_{i\downarrow}^c. \end{aligned} \quad (1)$$

where $d_{\mathbf{k}\sigma}^{\dagger}$ ($d_{\mathbf{k}\sigma}$) and $c_{\mathbf{k}\sigma}^{\dagger}$ ($c_{\mathbf{k}\sigma}$) are the creation (annihilation) operators for the more correlated orbital (d -orbital) and the less correlated c -orbitals, respectively. V is hybridization between d and c -orbitals, U_d and U_c are the on-site Coulomb repulsion for d and c -orbitals. Without loss of generality, here we consider equal intra-layer nearest-neighbor hopping for d and c -orbitals with $t_{\mathbf{k}}^d = t_{\mathbf{k}}^c = -2(\cos k_x + \cos k_y)$, which closely resemble the estimated value $t^{\text{Nd}}/t^{\text{Ni}} \approx 1.03$ in density functional theory (DFT) calculation for nickelates [46]. μ^d and μ^c are the corresponding chemical potentials. Unless specified, we use the doping for d -orbital $p = 1 - \langle n_d \rangle = 0.05$ and $U_d = 8$ throughout the paper.

To solve the above Hamiltonian, we use an eight-site cellular dynamical mean-field theory (CDMFT), which is a cluster extension of the dynamic mean-field theory (DMFT). The CDMFT method captures non-local correlations within the cluster exactly, while longer-range spatial correlations are dealt by a dynamical mean-field that embedded in an effective cluster impurity model [47, 48]. It is worth nothing that in CDMFT we do not make any presumption of the leading instability like in weak coupling approaches [49] or rescaling of electronic band structure in exchange model, which is crucial for mapping out the unconventional SC [47, 50, 51]. To solve the CDMFT impurity problem, we use the Hirsch-Fye quantum Monte Carlo solver [52] with a discrete time $\Delta\tau = 0.1$.

III. RESULT

A. Evolution from $d_{x^2-y^2}$ to s_{\pm} wave pairing

We investigate the pairing susceptibility [53–55] $\chi_{sc} \equiv \chi_{sc}^{dd,dd} = 1/N \sum_{i,j} \int_0^{\beta} \langle T_{\tau} P_j^{\dagger}(\tau) P_i(0) \rangle d\tau$, where $P_i =$

$(1/\sqrt{2})f(r)(d_{i,\uparrow}d_{i+r,\downarrow} - d_{i,\downarrow}d_{i+r,\uparrow})$ is the spin singlet pairing operator in the d -orbital, and $f(r)$ represents the d or s_{\pm} -wave form factor associated with a pairing bond r . In practice, here χ_{sc} is obtained by computing the linear pairing response of the system with a small pinning pairing field induced in Eq. (1). We first display the inverse pairing susceptibility χ_{sc}^{-1} as a function of temperature T for a series of different hybridization V in Fig. 1(a) ($d_{x^2-y^2}$ wave) and Fig. 1(b) (s_{\pm} wave). Here we use a typical set of parameters $U_d = 8, U_c = 4, n_d = 0.95, n_c = 0.9$. As one can see that at small V , χ_{sc}^{-1} of $d_{x^2-y^2}$ wave pairing decreases rapidly with lowering temperature T , which extrapolates to zero as approaching a finite temperature that we identify as the superconducting T_c . From Fig. 1, we see that as V increases, T_c of $d_{x^2-y^2}$ wave pairing decreases monotonously [56]. In contrast, for s_{\pm} wave the pairing instability first grows with V as $V \lesssim 2.5$, and T_c reaches its maximum at $V \sim 2.5$, then it quickly falls to zero as V approaching $V \sim 2.9$, see Fig. 1(b).

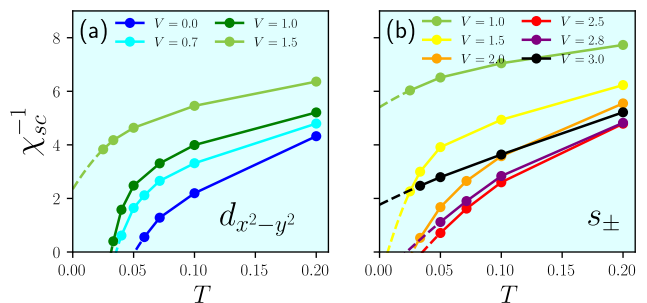


FIG. 1. The inverse pairing susceptibility χ_{sc}^{-1} as a function of T with varying V for (a) $d_{x^2-y^2}$ and (b) s_{\pm} wave pairings. The extending dashed curves at low T are quadratic interpolations.

Repeating above computations for different $\langle n_c \rangle$, U_c parameters, we obtain phase diagrams in Fig. 2(a), which display $d_{x^2-y^2}$ and s_{\pm} superconducting T_c as functions of V . The solid curves in the main plot show result for $U_c = 4$ (and $U_d = 8$), $\langle n_c \rangle = 0.8$, which reveals a clear evolution of the dominant pairing symmetry from $d_{x^2-y^2}$ to s_{\pm} wave as increasing V . Namely, for small V ($V \lesssim 1.0$), the $d_{x^2-y^2}$ pairing (dots) prevails, while for stronger hybridization $1.5 \lesssim V \lesssim 2.8$, the system becomes prone to s_{\pm} wave pairing (squares). Finally, when V is further increased, *i.e.*, when $V > 2.8$, the s_{\pm} wave T_c rapidly drops to zero, as localized singlets formed between d and c -electrons in a unit cell [40].

In addition to V , the pairing instabilities can also be sensitivity to the c -orbital density $\langle n_c \rangle$. To investigate the doping effects of c -orbital on SC, we compare the dashed lines ($\langle n_c \rangle = 0.8$) with the solid lines ($\langle n_c \rangle = 0.9$) in the main plot of Fig. 2, where one can see that changing c -density $\langle n_c \rangle$ does not significantly affect $d_{x^2-y^2}$ wave pairing, whereas the s_{\pm} pairing does demonstrate great variation to $\langle n_c \rangle$ [44, 45]. For example, at $V = 2.5$,

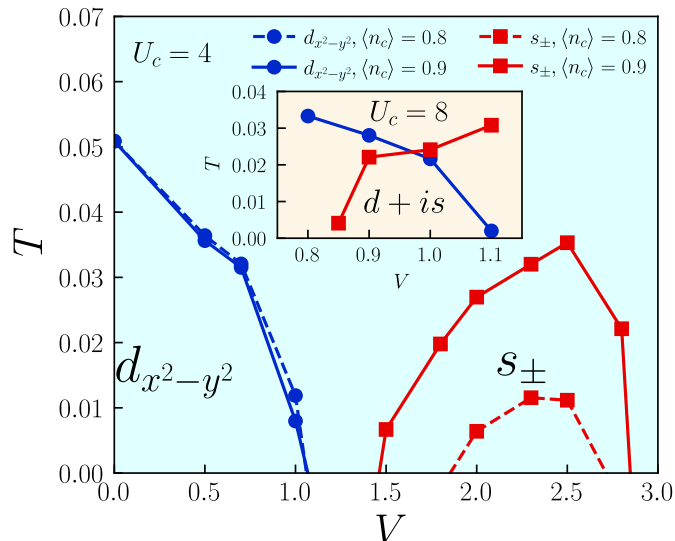


FIG. 2. T_c as a function of V for $n_c = 0.8$ (dashed lines) and 0.9 (solid lines) with $U_c = 4$ (cyan background). The $d_{x^2-y^2}$ and s_{\pm} wave pairings are marked by blue rounds and red squares. Inset: T_c as a function of V for $U_c = 8$ (light orange background), with $\langle n_c \rangle = 0.9$.

T_c of s_{\pm} wave pairing exhibits a drastic drop from 0.035 to 0.008 as $\langle n_c \rangle$ decreases from $\langle n_c \rangle = 0.9$ to $\langle n_c \rangle = 0.8$. In our study, when further decreasing $\langle n_c \rangle$, we could not find a finite T_c for s_{\pm} wave pairing in the temperature range that accessible to our study. To understand this remarkable difference in the dependence on $\langle n_c \rangle$ between $d_{x^2-y^2}$ and s_{\pm} wave pairing, we first note that for the $d_{x^2-y^2}$ wave pairing, it is typically associated with correlations between electrons effectively in a single band system [57]. Here we use $U_d = 8, U_c = 4$ such that the correlations effects in c -orbital is too weak to drive a $d_{x^2-y^2}$ wave instability (In CDMFT on single band Hubbard model, $U > 6$ is usually required to obtain superconductivity [58]). Thus the changing of n_c should not change much the $d_{x^2-y^2}$ wave pairing that caused by the d -electrons at small V . For the s_{\pm} wave pairing, since both d and c -orbitals are involved, the situation can be more complicated. Below we will tackle this problem from two aspects: (1) We study the changing of Fermi surface with V and n , which represents a typical low-energy property of the system that immediately affects the free energy of the pairing. (2) We employ the fluctuation diagnostics technique [59] to investigate the “pairing glue” between electrons that usually associated with higher energy aspect of the system.

Fig. 3 presents the interacting Fermi surface along with non-interacting FS shown in green lines. The upper panel in Fig. 3(a-c) is for smaller V cases, $V = 0.5, 0.7, 1.0$ where $d_{x^2-y^2}$ wave can be hosted at low T in this regime, and the lower panel in Fig. 3(d-f) is for larger V cases, $V = 1.5, 2.5, 3.0$ where s_{\pm} pairing occurs at low T in this regime. As one can see that, as increasing V , the

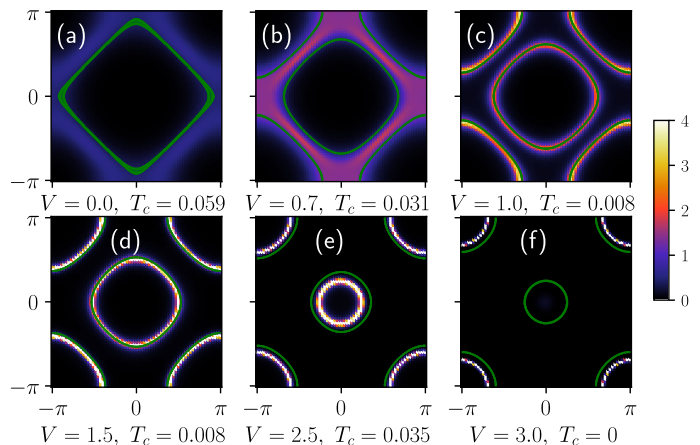


FIG. 3. Interacting Fermi surface in momentum space. (a-c) For small V in the $d_{x^2-y^2}$ pairing regime, with $V = 0.5, 0.7$ and 1.0 . Note that the $d_{x^2-y^2}$ wave T_c at these V is labeled in the respective plots. (d-f) For larger V in the s_{\pm} wave pairing regime, with $V = 1.5, 2.5$ and 3.0 . Here the dominant s_{\pm} wave T_c at these V are labeled in the respective plots. For reference, the green lines indicate the corresponding non-interacting FS. Here $\langle n_c \rangle = 0.9, U_c = 4, T = 1/30$.

FS as a whole evolves from diamond-like shape to a well separated electron-pocket/ hole-pocket structure. This is generally in accordance with the evolving of the pairing symmetry from $d_{x^2-y^2}$ to s_{\pm} wave, as the former prefers a diamond-like Fermi surface to minimize the free energy, the latter is more associated with pairing electrons scattered between electron and hole pockets [60]. There are a couple of points we would like to stress on: (1) Putting aside the blur (continuum) between $d - c$ bands in momentum space at small V , generally speaking, interaction does not change much the shape or loci of the Fermi surface at large V . In the zero V (or the single-band) limit, the shape of the Fermi surface can be strongly renormalized at small dopings, due to the particle-hole asymmetry in the electron scattering [61]. Here we see that for $V \geq 0.7$, in contrast, the interacting Fermi surface is in generally outlined by its non-interacting counterpart. (2) In the intermediate V regime, *i.e.*, $V \sim 1.0$ in Fig. 3(c), the geometry of the Fermi surface in principle allows both $d_{x^2-y^2}$ and s_{\pm} wave pairing with minimized free energies. In other words, for both gap functions $\Delta(\mathbf{k})$, there is a large overlap between the non-zero $\Delta(\mathbf{k})$ and the Fermi surface [60], which makes the pairing energetically possible. Moreover, here scattering of electrons within the same band or between the two different bands are both feasible, which does not prevent the the form of $d_{x^2-y^2}$ or s_{\pm} wave Cooper pairs. However, in our study we in fact did not detect the sign of the coexistence of $d_{x^2-y^2}$ and s_{\pm} pairing in this parameter regime. Namely, here we only found a finite T_c for $d_{x^2-y^2}$ wave pairing, but no finite T_c for s_{\pm} pairing is seen in the temperature range accessible to us. As we will show below, the value of U_c is critical to the formation of s_{\pm} pairing at intermedi-

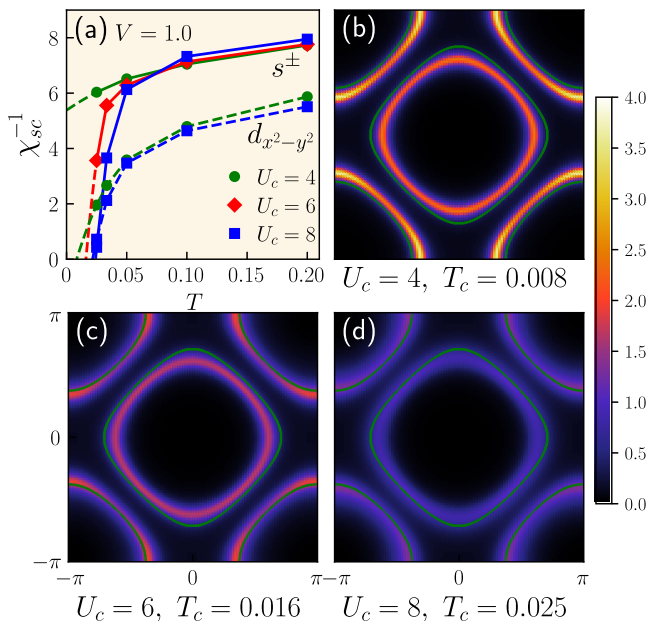


FIG. 4. (a) The inverse pairing susceptibility χ_{sc}^{-1} as a function of T with varying U_c for d (dashed lines) and s_{\pm} wave (solid lines) pairing. (b-d) FS with $U_c = 4, 6, 8$. For reference, the green lines indicate non-interacting FS. Here $V = 1.0$, $\langle n_c \rangle = 0.9$ and $U_c = 8$, $T = 1/30$ are used.

ate V ($V \sim 1$). We found that only when $U_c \gtrsim 6$, a finite T_c for s_{\pm} pairing can be reached at $V \sim 1.0$. This suggests that, besides the Fermi surface geometry, other ingredients like the subtle change of Hubbard U between electrons are also crucial in driving the s_{\pm} pairing instability.

Above we have shown results for $\langle n_c \rangle = 0.9$ in Fig. 3. One may expect that the strong $\langle n_c \rangle$ dependence of s_{\pm} wave pairing shown in Fig. 2 could also manifest in the $\langle n_c \rangle$ dependence of FS topology, since decreasing $\langle n_c \rangle$ results in the shrink of electron pocket and the expansion of hole pocket in a way disfavoring s_{\pm} pairing. Here we have verified that such FS deformation is in fact marginal (no shown). We argue that the detrimetal effect on s_{\pm} pairing by decreasing $\langle n_c \rangle$ is due to the fact that decreasing $\langle n_c \rangle$ leads to the diminishing of the direct magnetic exchange on the $d-c$ bonds that scales like $V^2/(U_d+U_c)$ when d and c -orbitals are both close to half-filling. See also below the fluctuation diagnostics on the pairing glue of s_{\pm} wave.

B. Coexisting $d + is$ wave with interactions

In the above study, we found that $U_c = 4$ is insufficient to stabilize a coexisting $d_{x^2-y^2}$ and s_{\pm} wave pairing at different $\langle n_c \rangle$ and V . However, by increasing U_c up to 8, we did detect the coexistence of $d_{x^2-y^2}$ and s_{\pm} wave pairing at the intermediate V . In order to determine the T_c for both pairing symmetries, here we separately com-

pute the $d_{x^2-y^2}$ and s_{\pm} wave pairing susceptibility for each parameter point during the DMFT self-consistent loops. In Fig. 4(a), we plot χ_{sc}^{-1} as a function of T for both $d_{x^2-y^2}$ and s_{\pm} wave at $V = 1.0$. One clearly sees that, as increasing U_c , χ_{sc} is drastically enhanced for s_{\pm} wave at low T , while the $d_{x^2-y^2}$ wave pairing susceptibility is affected more in a quantitative way. In particular, as $U_c = 4$ is increased to $U_c = 6$, a finite T_c for s_{\pm} wave pairing is reached, which signals the onset of the coexisting phase, as T_c for $d_{x^2-y^2}$ wave is always finite in this parameter regime (dashed lines).

Our results on the coexistence of $d_{x^2-y^2}$ and s_{\pm} wave for $V \in (0.8 - 1.1)$, $U_c = 8$ can be summarized in the driven of Fig. 2, which exhibits a phase diagram featuring the coexistence of $d_{x^2-y^2}$ and s_{\pm} wave pairings. Comparing with $U_c = 4$ result in the main plot, the s_{\pm} wave instability in the driven at $U_c = 8$ is enormously enhanced. For example, at $U_c = 4$, the minimal V for s_{\pm} wave is around $V_{min} \sim 1.5$, while at $U_c = 8$ it is significantly reduced to $V_{min} \sim 0.85$. For $d_{x^2-y^2}$ wave, the T_c is also notably enhanced with increasing U_c , for example, for $V = 1.0$, $T_c \approx 0.008$ at $U_c = 4$ (main plot) while $T_c \approx 0.02$ at $U_c = 8$ (Inset). To summarize, at $V \sim 1$, $d_{x^2-y^2}$ and s_{\pm} pairing have a comparable superconducting T_c , $T_c \approx 0.025$. As V increases, T_c of s_{\pm} increases and that of $d_{x^2-y^2}$ decreases, and otherwise the opposite.

When focusing on the FS evolution in Fig. 4(b-d), we found that such triggering effects on increasing U_c is rarely reflected in FS geometry. Here, increasing U_c only leads to a slight broadening of FS profile. This result also confirms our aforementioned argument that the role of FS is less important for s_{\pm} wave pairing.

C. Fluctuation diagnostics

To unveil the driving forces for SC instabilities, here we apply fluctuation diagnostics [59, 62]. The essential idea of this approach is to use the Schwinger-Dyson equation of motion (SDEOM) to decompose the self-energies into a summation of various two-particle Green's functions. It has been recently used to reveal the significance of collective fluctuations in the formation of d wave superconductivity [63], pseudogap [59], and strange metal state [64]. Here we will focus on the fluctuation diagnostics in the parameter regime of $d + is$ wave pairing. In the magnetic (spin) channel, SDEOM of self-energy can be expressed as

$$[\Sigma G]_{(m\alpha, n\beta)}^{\mathbf{k}} = -\frac{U_m}{N^2} \sum_{\mathbf{k}' \mathbf{q}} G^2(\mathbf{k}' + \mathbf{q}m\bar{\alpha}, \mathbf{k} + \mathbf{q}m\bar{\alpha}, \mathbf{k}'m\alpha, \mathbf{k}n\beta), \quad (2)$$

in which $G^2(ijkl) = \langle \mathcal{T} c_i^\dagger c_j c_k c_l^\dagger \rangle$, \mathbf{k}, \mathbf{k}' denote fermionic momenta/frequencies, and \mathbf{q} represents momentum transfer/bosonic frequency, m, n denote orbital indices and α, β are spin indices. Dividing the full Green's function matrix G on both sides of above equation, and sum

over \mathbf{k}' , we can obtain the self-energy as the sum of four different fractions like

$$\Sigma(\mathbf{k}) = \sum_{\mathbf{q}} [\Sigma_{\mathbf{q}}^{M,dd} + \Sigma_{\mathbf{q}}^{M,dc} + \Sigma_{\mathbf{q}}^{X,dd} + \Sigma_{\mathbf{q}}^{X,dc}] (\mathbf{k}). \quad (3)$$

Here $\Sigma_{\mathbf{q}}^{M,mn}(\mathbf{k})$ acquires a physical meaning that the relative weight of $\Sigma_{\mathbf{q}}^{M,mn}(\mathbf{k})$ at different \mathbf{q} denotes the importance of the magnetic fluctuation with transfer momentum \mathbf{q} in depleting electrons with momentum \mathbf{k} , since $\Sigma_{\mathbf{q}}^{M,mn} \propto \langle S_m^+(\mathbf{q}) S_n^-(\mathbf{-q}) \rangle$ [64], while $\Sigma_{\mathbf{q}}^{X,mn}$ is the fraction that beyond the description of magnetic fluctuations, which can be alternatively seen as the fluctuation between the spin and particle-particle (pairing) degrees of freedom: $\Sigma_{\mathbf{q}}^{X,mn} \propto \langle \Delta_m(\mathbf{q}) S_n^-(\mathbf{-q}) \rangle$, with triplet pairing operator $\Delta_m(\mathbf{q}) = \sum_{\mathbf{k}} (c_{m\mathbf{k}\downarrow} c_{m\mathbf{q}-\mathbf{k}\downarrow})$. In our study, we find that $\Sigma_{\mathbf{q}}^{X,mn}$ are either negligible (for $d_{x^2-y^2}$ wave) or only have negative contributions (pair-breaking, for s_{\pm} wave). Hence below we only discuss the $\Sigma_{\mathbf{q}}^{M,mn}(\mathbf{k})$ contributions. In addition, here dd or dc denotes the contribution from the fluctuations inside d -layer or between the $d-c$ layers. We stress that the above sum rule in Eq. (3) of fluctuation diagnostics is exact without any approximation.

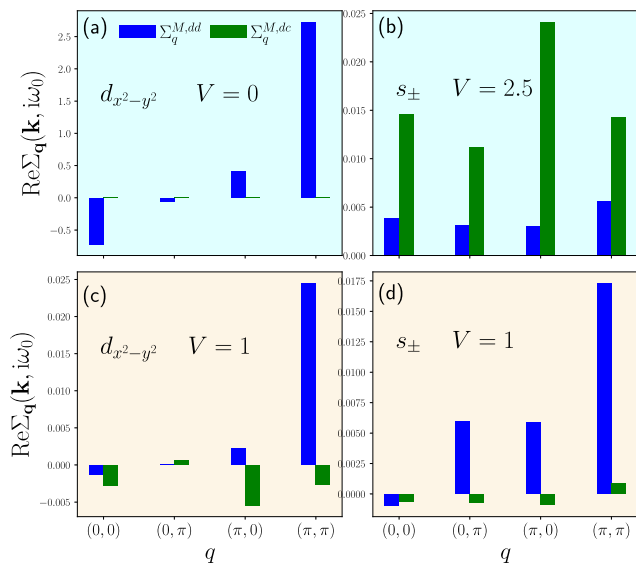


FIG. 5. (a) The fluctuation diagnostics of the anomalous self-energies $\text{Re}\Sigma_{\mathbf{q}}^{M,dd/dc}(\mathbf{k}, i\omega_0)$ as a function of transfer momentum \mathbf{q} in the magnetic channel. (a) $d_{x^2-y^2}$ wave pairing for $\mathbf{k} = (0, \pi)$, $V = 0$. (b) s_{\pm} wave pairing for $\mathbf{k} = (0, 0)$, $V = 2.5$. (c) $d_{x^2-y^2}$ and (d) s_{\pm} wave pairing for $V = 1, U_c = 8$. The temperature $T = 1/30$.

Since we are most interested in the superconductivity, which is encoded in the real part of anomalous self-energies. Focusing on the low-energy physics, we study the anomalous self-energies at the first Matsubara frequency $\text{Re}\Sigma_{\mathbf{q}}(\mathbf{k}, i\omega_0)$. In Fig. 5, we show the fluctuation diagnostics as a function of \mathbf{q} , with $T = 1/30$. Fig. 5(a-b) respectively show $V = 0$ and 2.5 with $U_c = 4$. In

Fig. 5(a), $\Sigma_{\mathbf{q}}^{M,dc}$ (blue) has zero weight due to the decoupling of $d-c$ layers at $V = 0$, in this case a predominated $\Sigma_{(\pi,\pi)}^{M,dd}$ at $\mathbf{q} = (\pi, \pi)$ overwhelms that of all others q , highlighting the antiferromagnetic fluctuation origin of the $d_{x^2-y^2}$ pairing in a single band system [63]. In Fig. 5(b) where s_{\pm} wave prevails, the major contributions are from inter-layer $\Sigma_{\mathbf{q}}^{M,dc}$ (green) which are quite evenly distributed among four different \mathbf{q} , suggesting that here the anomalous self-energy, or the source of the pairing, should be seen as mainly stemming from the antiferromagnetic fluctuations between the local $d-c$ bond in real space. Fig. 5(c-d) respectively display the result for $d_{x^2-y^2}$ and s_{\pm} wave pairing in the $d+is$ coexistence regime at the intermediate V . Comparing Fig. 5(c) with Fig. 5(a), although the absolute magnitude of $\Sigma_{(\pi,\pi)}^{M,dd}$ (blue) is enormously depressed, the $\mathbf{q} = (\pi, \pi)$ mode retains its predominant role in anomalous scatterings, which again emphasizes the vital role of antiferromagnetic fluctuations in $d_{x^2-y^2}$ wave pairing. However for Fig. 5(d), the situation is quite different as compared with Fig. 5(b). Here the fluctuation decomposition shows a major contribution from $\Sigma_{\mathbf{q}}^{M,dd}$. In fact we find the magnitude of $\Sigma_{\mathbf{q}}^{X,dd}$ is almost as strong as $\Sigma_{\mathbf{q}}^{M,dd}$ but with the opposite signs (not shown here), which means they cancel out with each other ($\sum_{\mathbf{q}} [\Sigma_{\mathbf{q}}^{M,dd} + \Sigma_{\mathbf{q}}^{X,dd}] \approx 0$). In this case another positive contribution from $\Sigma_{(\pi,\pi)}^{X,dc}$, although not as significant as the former two, is however not negligible for the s_{\pm} wave pairing (no shown). These further suggest that the fluctuations of the s_{\pm} wave in the coexistence regime is rather complicated and can not be simply attributed to a specific magnetic fluctuation channel based on the fluctuation diagnostics.

IV. DISCUSSION

In our systematic investigation, we have shown that for the $d_{x^2-y^2}$ wave pairing of strongly correlated electrons, when a second band with a small U is introduced, the hybridization effects between the bands will effectively suppress the superconducting T_c . This may can be understand from two aspects. First, the hybridization changes the geometry of the Fermi surface to energetically disfavor the $d_{x^2-y^2}$ wave form factor. Secondly, the less correlated electrons from the second band can screen the localized electrons in the strongly correlated band, by suppressing the intra-band antiferromagnetic exchanges. Therefore, a multi-orbital description of nickelates involving the $5d$ -orbitals would inevitably lead to the suppression of $d_{x^2-y^2}$ wave pairing [65]. In experiments, a recent resonant inelastic x-ray scattering study [66] reveals that the Ni- $3d$ electrons in the ground state of the undoped NdNiO₂ is an antiferromagnetically aligned with substantial damping, due to the coupling to rare-earth itinerant electrons.

Our study also demonstrates that the coexistence of $d_{x^2-y^2}$ and s_{\pm} wave, or the $d+is$ wave pairing is quite

elusive in a two-band system, which requires a large electron repulsion in the c -orbital and an intermediate hybridization $V \sim t$. Regarding the nickelate materials, recent experimental evidences have shown that the effective hybridization between Ni-3d and Nd-derived orbitals is essentially small [27, 65, 67–69]. Moreover, considering also the itinerant carrier density $\langle n_c \rangle$ is estimated to be only 0.08 per unit cell [7], which is one order of magnitude smaller than our estimation for a finite T_c for s_{\pm} wave pairing. Therefore, we conjecture that the potential s_{\pm} wave, as well as the coexisting $d+is$ wave pairing, would have an extremely small T_c , if it ever exists in infinite layer nickelates. We note that in the tunneling experiment [9], the $d_{x^2-y^2}$ V-shaped gap is reported to be an intrinsic feature in the infinite layer nickelates, while U-shaped s_{\pm} wave gap seems more associated with a rough surface. In London penetration experiments, $d+is$ wave pairing was also reported [17], where the full gap, however, was also argued to be attributed to the magnetic impurities [18].

V. CONCLUSION

In summary, we have established a phase diagram of $d_{x^2-y^2}$, s_{\pm} and $d+is$ wave pairing in a two-orbital Hubbard model, in which we clarify the roles of hybridization (V), itinerant carrier density ($\langle n_c \rangle$) and Hubbard interaction (U_c) in determining the superconducting T_c . Our study have demonstrated that the entrance of the 5d-electrons at Fermi level hazards the $d_{x^2-y^2}$ wave pairing in the Ni-3d orbital. On the other hand, the two-orbital $d+is$ wave pairing, however, requires a relative large Coulomb repulsion in the 5d-orbital. We have also performed the fluctuation diagnostics to reveal the driving force behind the $d_{x^2-y^2}$ and s_{\pm} wave pairing in this system. Our study overall supports an intrinsic $d_{x^2-y^2}$ wave pairing in the nickelate superconductors despite the contamination of rare-earth derived bands at the Fermi level.

ACKNOWLEDGMENTS

We are grateful to Mi Jiang for useful discussions. This project was supported by the National Key Research and Development Program of China (Grant No. 2022YFA1402802), the National Natural Science Foundation of China (Grants No. 12274472, No. 92165204, No. 11974432,), Shenzhen International Quantum Academy (Grant No. SIQA202102), and GuangZhou National supercomputing center.

-
- [1] P. A. Lee, N. Nagaosa, and X.-G. Wen, *Reviews of Modern Physics* **78**, 17 (2006).
- [2] W. C. Lee, S. C. Zhang, and C. Wu, *Phys Rev Lett* **102**, 217002 (2009).
- [3] R. M. Fernandes and A. J. Millis, *Physical Review Letters* **111** (2013), 10.1103/physrevlett.111.127001.
- [4] C. Platt, R. Thomale, C. Honerkamp, S.-C. Zhang, and W. Hanke, *Physical Review B* **85** (2012), 10.1103/PhysRevB.85.180502.
- [5] T. A. Maier, S. Graser, P. J. Hirschfeld, and D. J. Scalapino, *Physical Review B* **83** (2011), 10.1103/PhysRevB.83.100515.
- [6] D. Li, K. Lee, B. Y. Wang, M. Osada, S. Crossley, H. R. Lee, Y. Cui, Y. Hikita, and H. Y. Hwang, *Nature* **572**, 624 (2019).
- [7] D. Li, B. Y. Wang, K. Lee, S. P. Harvey, M. Osada, B. H. Goodge, L. F. Kourkoutis, and H. Y. Hwang, *Physical Review Letters* **125** (2020), 10.1103/physrevlett.125.027001.
- [8] S. Zeng, C. S. Tang, X. Yin, C. Li, M. Li, Z. Huang, J. Hu, W. Liu, G. J. Omar, H. Jani, Z. S. Lim, K. Han, D. Wan, P. Yang, S. J. Pennycook, A. T. Wee, and A. Ariando, *Physical Review Letters* **125** (2020), 10.1103/physrevlett.125.147003.
- [9] Q. Gu, Y. Li, S. Wan, H. Li, W. Guo, H. Yang, Q. Li, X. Zhu, X. Pan, Y. Nie, and H.-H. Wen, *Nature Communications* **11** (2020), 10.1038/s41467-020-19908-1.
- [10] M. Osada, B. Y. Wang, B. H. Goodge, K. Lee, H. Yoon, K. Sakuma, D. Li, M. Miura, L. F. Kourkoutis, and H. Y. Hwang, *Nano Letters* **20**, 5735 (2020).
- [11] M. Osada, B. Y. Wang, K. Lee, D. Li, and H. Y. Hwang, *Physical Review Materials* **4** (2020), 10.1103/PhysRevMaterials.4.121801.
- [12] X.-R. Zhou, Z.-X. Feng, P.-X. Qin, H. Yan, X.-N. Wang, P. Nie, H.-J. Wu, X. Zhang, H.-Y. Chen, Z.-A. Meng, Z.-W. Zhu, and Z.-Q. Liu, *Rare Metals* (2021), 10.1007/s12598-021-01768-3.
- [13] G. A. Pan, D. F. Segedin, H. LaBollita, Q. Song, E. M. Nica, B. H. Goodge, A. T. Pierce, S. Doyle, S. Novakov, D. C. Carrizales, A. T. N'Diaye, P. Shafer, H. Paik, J. T. Heron, J. A. Mason, A. Yacoby, L. F. Kourkoutis, O. Erten, C. M. Brooks, A. S. Botana, and J. A. Mundy, *Nature Materials* (2021).
- [14] M. Osada, B. Y. Wang, B. H. Goodge, S. P. Harvey, K. Lee, D. Li, L. F. Kourkoutis, and H. Y. Hwang, *Adv Mater* **33**, e2104083 (2021).
- [15] S. Zeng, C. Li, L. E. Chow, Y. Cao, Z. Zhang, C. S. Tang, X. Yin, Z. S. Lim, J. Hu, P. Yang, and A. Ariando, *Science Advances* **8**, eabl9927 (2022), <https://www.science.org/doi/pdf/10.1126/sciadv.abl9927>.
- [16] S. W. Zeng, X. M. Yin, C. J. Li, L. E. Chow, C. S. Tang, K. Han, Z. Huang, Y. Cao, D. Y. Wan, Z. T. Zhang, Z. S. Lim, C. Z. Diao, P. Yang, A. T. S. Wee, S. J. Pennycook, and A. Ariando, *Nat Commun* **13**, 743 (2022).

- [17] L. E. Chow, S. K. Sudheesh, Z. Y. Luo, P. Nandi, T. Heil, J. Deuschle, S. W. Zeng, Z. T. Zhang, S. Prakash, X. M. Du, Z. S. Lim, P. A. van Aken, E. E. M. Chia, and A. Ariando, “Pairing symmetry in infinite-layer nickelate superconductor,” (2023), [arXiv:2201.10038 \[cond-mat.supr-con\]](https://arxiv.org/abs/2201.10038).
- [18] S. P. Harvey, B. Y. Wang, J. Fowlie, M. Osada, K. Lee, Y. Lee, D. Li, and H. Y. Hwang, “Evidence for nodal superconductivity in infinite-layer nickelates,” (2022).
- [19] Z. Wang, G.-M. Zhang, Y.-F. Yang, and F.-C. Zhang, *Physical Review B* **102** (2020), [10.1103/physrevb.102.220501](https://doi.org/10.1103/physrevb.102.220501).
- [20] J. Zaanen, G. A. Sawatzky, and J. W. Allen, *Phys. Rev. Lett.* **55**, 418 (1985).
- [21] M. Jiang, M. Berciu, and G. A. Sawatzky, *Phys Rev Lett* **124**, 207004 (2020).
- [22] E. Been, W.-S. Lee, H. Y. Hwang, Y. Cui, J. Zaanen, T. Devereaux, B. Moritz, and C. Jia, *Phys. Rev. X* **11**, 011050 (2021).
- [23] M. Hepting, D. Li, C. J. Jia, H. Lu, E. Paris, Y. Tseng, X. Feng, M. Osada, E. Been, Y. Hikita, Y. D. Chuang, Z. Hussain, K. J. Zhou, A. Nag, M. Garcia-Fernandez, M. Rossi, H. Y. Huang, D. J. Huang, Z. X. Shen, T. Schmitt, H. Y. Hwang, B. Moritz, J. Zaanen, T. P. Devereaux, and W. S. Lee, *Nat Mater* **19**, 381 (2020).
- [24] A. S. Botana and M. R. Norman, *Physical Review X* **10** (2020), [10.1103/PhysRevX.10.011024](https://doi.org/10.1103/PhysRevX.10.011024).
- [25] G.-M. Zhang, Y.-f. Yang, and F.-C. Zhang, *Physical Review B* **101** (2020), [10.1103/PhysRevB.101.020501](https://doi.org/10.1103/PhysRevB.101.020501).
- [26] B. H. Goodge, D. Li, K. Lee, M. Osada, B. Y. Wang, G. A. Sawatzky, H. Y. Hwang, and L. F. Kourkoutis, *Proc Natl Acad Sci U S A* **118** (2021), [10.1073/pnas.2007683118](https://doi.org/10.1073/pnas.2007683118).
- [27] F. Petocchi, V. Christiansson, F. Nilsson, F. Aryasetiawan, and P. Werner, *Physical Review X* **10** (2020), [10.1103/PhysRevX.10.041047](https://doi.org/10.1103/PhysRevX.10.041047).
- [28] I. Leonov, S. L. Skornyakov, and S. Y. Savrasov, *Physical Review B* **101** (2020), [10.1103/physrevb.101.241108](https://doi.org/10.1103/physrevb.101.241108).
- [29] J. Karp, A. S. Botana, M. R. Norman, H. Park, M. Zingl, and A. Millis, *Physical Review X* **10** (2020), [10.1103/physrevx.10.021061](https://doi.org/10.1103/physrevx.10.021061).
- [30] F. Lechermann, *Physical Review X* **10** (2020), [10.1103/PhysRevX.10.041002](https://doi.org/10.1103/PhysRevX.10.041002).
- [31] F. Lechermann, *Physical Review B* **101** (2020), [10.1103/PhysRevB.101.081110](https://doi.org/10.1103/PhysRevB.101.081110).
- [32] F. Lechermann, *Physical Review Materials* **5** (2021), [10.1103/physrevmaterials.5.044803](https://doi.org/10.1103/physrevmaterials.5.044803).
- [33] J. Hu and H. Ding, *Scientific Reports* **2** (2012), [10.1038/srep00381](https://doi.org/10.1038/srep00381).
- [34] N. Bulut, D. J. Scalapino, and R. T. Scalettar, *Phys Rev B Condens Matter* **45**, 5577 (1992).
- [35] R. E. Hetzel, W. von der Linden, and W. Hanke, *Phys Rev B Condens Matter* **50**, 4159 (1994).
- [36] R. T. Scalettar, J. W. Cannon, D. J. Scalapino, and R. L. Sugar, *Phys Rev B Condens Matter* **50**, 13419 (1994).
- [37] R. R. dos Santos, *Phys Rev B Condens Matter* **51**, 15540 (1995).
- [38] K. Bouadim, G. G. Batrouni, F. Hébert, and R. T. Scalettar, *Physical Review B* **77** (2008), [10.1103/PhysRevB.77.144527](https://doi.org/10.1103/PhysRevB.77.144527).
- [39] S. S. Kancharla and S. Okamoto, *Physical Review B* **75** (2007), [10.1103/PhysRevB.75.193103](https://doi.org/10.1103/PhysRevB.75.193103).
- [40] T. A. Maier and D. J. Scalapino, *Physical Review B* **84** (2011), [10.1103/physrevb.84.180513](https://doi.org/10.1103/physrevb.84.180513).
- [41] V. Mishra, D. J. Scalapino, and T. A. Maier, *Sci Rep* **6**, 32078 (2016).
- [42] M. Nakata, D. Ogura, H. Usui, and K. Kuroki, *Physical Review B* **95** (2017), [10.1103/PhysRevB.95.214509](https://doi.org/10.1103/PhysRevB.95.214509).
- [43] T. A. Maier, V. Mishra, G. Balduzzi, and D. J. Scalapino, *Physical Review B* **99** (2019), [10.1103/PhysRevB.99.140504](https://doi.org/10.1103/PhysRevB.99.140504).
- [44] S. Karakuzu, S. Johnston, and T. A. Maier, *Physical Review B* **104** (2021), [10.1103/PhysRevB.104.245109](https://doi.org/10.1103/PhysRevB.104.245109).
- [45] E. M. Nica and O. Erten, *Physical Review B* **102** (2020), [10.1103/PhysRevB.102.214509](https://doi.org/10.1103/PhysRevB.102.214509).
- [46] X. Wu, K. Jiang, D. D. Sante, W. Hanke, A. P. Schnyder, J. Hu, and R. Thomale, “Surface *s*-wave superconductivity for oxide-terminated infinite-layer nickelates,” (2020), [arXiv:2008.06009 \[cond-mat.supr-con\]](https://arxiv.org/abs/2008.06009).
- [47] T. A. Maier, *Reviews of Modern Physics* **77** (2005).
- [48] T. A. Maier, M. Jarrell, T. C. Schulthess, P. R. C. Kent, and J. B. White, *Phys. Rev. Lett.* **95**, 237001 (2005).
- [49] R. M. Fernandes and A. V. Chubukov, *Rep Prog Phys* **80**, 014503 (2017).
- [50] A. Georges, *Reviews of Modern Physics* **68** (1996).
- [51] G. Kotliar, S. Y. Savrasov, G. Pálsson, and G. Biroli, *Physical Review Letters* **87** (2001), [10.1103/physrevlett.87.186401](https://doi.org/10.1103/physrevlett.87.186401).
- [52] J. E. Hirsch and R. M. Fye, *Phys Rev Lett* **56**, 2521 (1986).
- [53] N. Lin, E. Gull, and A. J. Millis, *Phys Rev Lett* **109**, 106401 (2012).
- [54] A. M. Black-Schaffer, W. Wu, and K. Le Hur, *Physical Review B* **90** (2014), [10.1103/PhysRevB.90.054521](https://doi.org/10.1103/PhysRevB.90.054521).
- [55] W. Wu and A.-M.-S. Tremblay, *Physical Review X* **5** (2015), [10.1103/physrevx.5.011019](https://doi.org/10.1103/physrevx.5.011019).
- [56] M. Jiang, “Characterizing the superconducting instability in a two-orbital *d-s* model: insights to infinite-layer nickelate superconductors,” (2022), [arXiv:2201.12967 \[cond-mat.supr-con\]](https://arxiv.org/abs/2201.12967).
- [57] F. C. Zhang and T. M. Rice, *Phys. Rev. B* **37**, 3759 (1988).
- [58] L. Fratino, P. Sémon, G. Sordi, and A.-M. S. Tremblay, *Scientific Reports* **6**, 22715 (2016).
- [59] O. Gunnarsson, T. Schafer, J. P. LeBlanc, E. Gull, J. Merino, G. Sangiovanni, G. Rohringer, and A. Toschi, *Phys Rev Lett* **114**, 236402 (2015).
- [60] J. Hu and H. Ding, *Scientific Reports* **2** (2012), [10.1038/srep00381](https://doi.org/10.1038/srep00381).
- [61] W. Wu, M. S. Scheurer, S. Chatterjee, S. Sachdev, A. Georges, and M. Ferrero, *Physical Review X* **8** (2018), [10.1103/PhysRevX.8.021048](https://doi.org/10.1103/PhysRevX.8.021048).
- [62] T. Schafer and A. Toschi, *J Phys Condens Matter* **33** (2021), [10.1088/1361-648X/abeb44](https://doi.org/10.1088/1361-648X/abeb44).
- [63] X. Dong, L. D. Re, A. Toschi, and E. Gull, *Proceedings of the National Academy of Sciences* **119**, e2205048119 (2022), <https://www.pnas.org/doi/pdf/10.1073/pnas.2205048119>.
- [64] W. Wu, X. Wang, and A. M. Tremblay, *Proc Natl Acad Sci U S A* **119**, e2115819119 (2022).
- [65] X. Wu, D. Di Sante, T. Schwemmer, W. Hanke, H. Y. Hwang, S. Raghu, and R. Thomale, *Phys. Rev. B* **101**, 060504 (2020).
- [66] H. Lu, M. Rossi, A. Nag, M. Osada, D. F. Li, K. Lee, B. Y. Wang, M. Garcia-Fernandez, S. Agrestini, Z. X. Shen, E. M. Been, B. Moritz, T. P. Devereaux, J. Zaanen, H. Y. Hwang, K. J. Zhou, and W. S. Lee, *Science* **373**, 213 (2021).

- [67] H. Zhang, L. Jin, S. Wang, B. Xi, X. Shi, F. Ye, and J.-W. Mei, *Physical Review Research* **2** (2020), [10.1103/physrevresearch.2.013214](https://doi.org/10.1103/physrevresearch.2.013214).
- [68] M.-Y. Choi, K.-W. Lee, and W. E. Pickett, *Physical Review B* **101** (2020), [10.1103/PhysRevB.101.020503](https://doi.org/10.1103/PhysRevB.101.020503).
- [69] J. Huang, R. Yu, Z. Xu, J.-X. Zhu, J. S. Oh, Q. Jiang, M. Wang, H. Wu, T. Chen, J. D. Denlinger, S.-K. Mo, M. Hashimoto, M. Michiardi, T. M. Pedersen, S. Gorovikov, S. Zhdanovich, A. Damascelli, G. Gu, P. Dai, J.-H. Chu, D. Lu, Q. Si, R. J. Birgeneau, and M. Yi, *Communications Physics* **5** (2022), [10.1038/s42005-022-00805-6](https://doi.org/10.1038/s42005-022-00805-6).